Date: April 21, 2003

Dijet Production at low Bjorken-*x* in Deep-Inelastic Scattering

H1 Collaboration

Abstract

Dijet production in deep-inelastic ep scattering is investigated in the regime of low values of the Bjorken-variable x ($10^{-4} < x < 10^{-2}$) and low four-momentum transfers Q^2 ($5 < Q^2 < 100$ GeV^2). The resulting dijet cross sections are compared to perturbative QCD calculations in next-to-leading order. For most dijet variables studied, these calculations can provide a reasonable description of the data over almost the full phase space region covered, including the regime of very low x. However, striking differences are observed for events with small azimuthal jet separation, an observable sensitive to the transverse momentum of the incoming gluon. They are most striking for the NLO calculations, but predictions based on the CCFM evolution equation, which incorporate the ideas of k_t factorization and the concept of unintegrated parton distributions, and which should be particularly suited for low x, also fail to describe the data. A better but not good description of the data is provided by various leading order Monte Carlo programs which differ mainly in the way they model higher order effects through parton cascades.

Preliminary results for DIS03, St. Petersburg

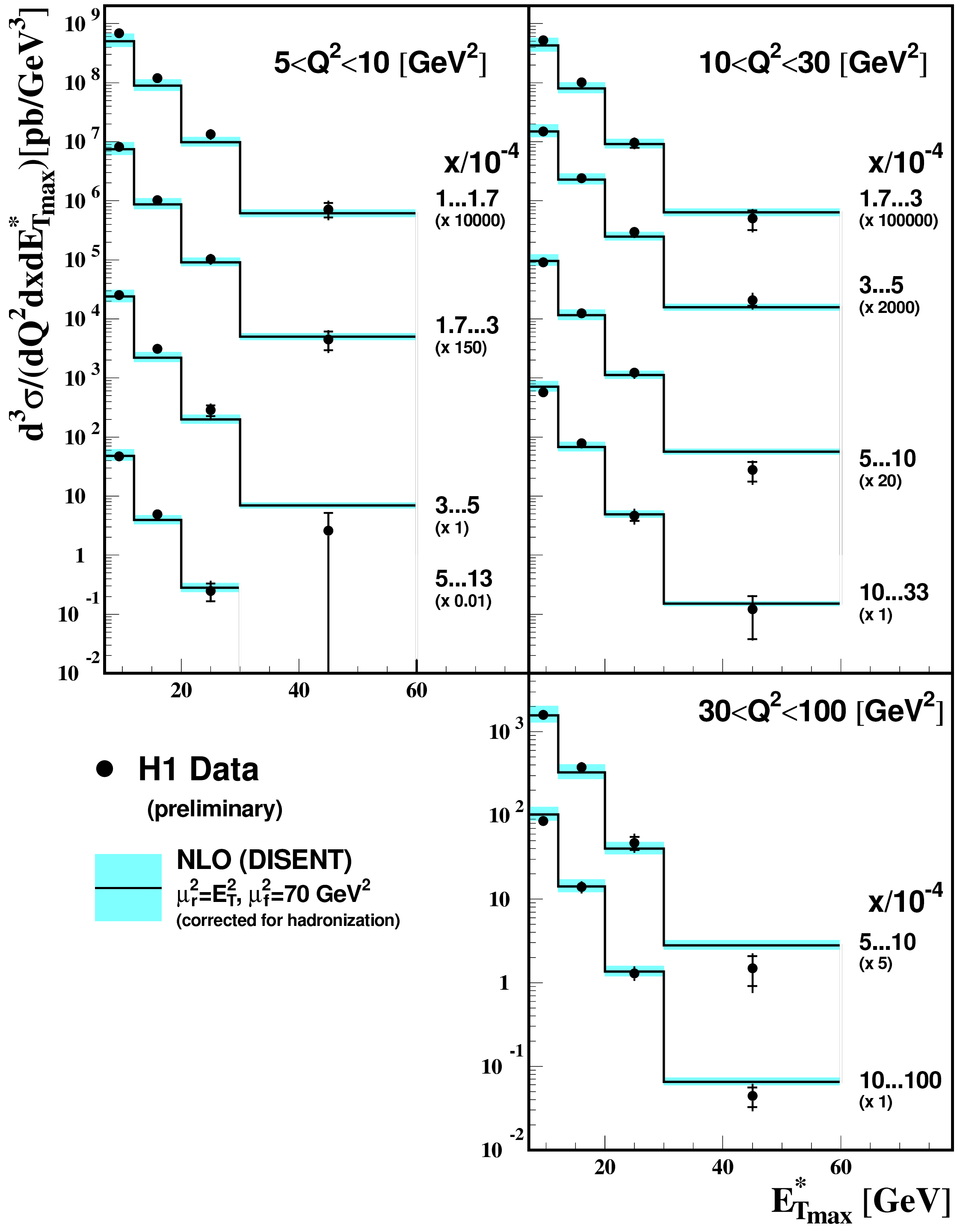

Figure 1: The triple differential inclusive dijet cross section in bins of Bjorken-x and Q^2 as a function of the jet-$E^*_{T,\max}$ compared to NLO QCD predictions using the CTEQ6M parton distribution functions. The data are shown together with their statistical (inner error bars) and their statistical and systematic error bars added in quadrature (outer error bars). The NLO predictions are corrected for hadronization effects which lower the pure theoretical prediction by $\approx 10\%$. The error band given for the NLO predictions includes the quadratic sum of hadronization and renormalization scale uncertainties.

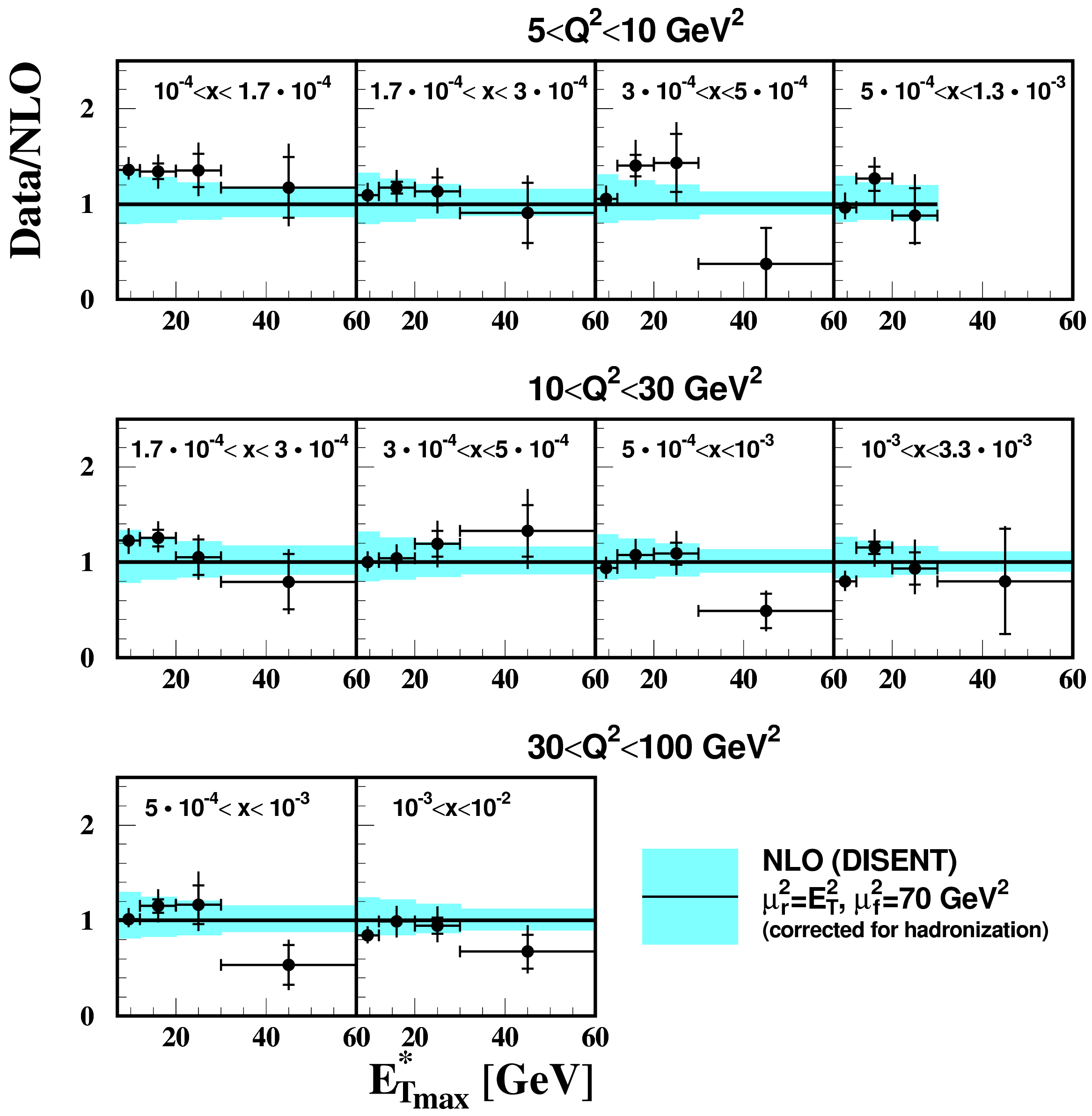

Figure 2: The ratio of the measured triple differential inclusive dijet cross section as a function of the jet-$E^*_{T,\max}$ and the NLO QCD predictions using the CTEQ6M parton distribution functions. The uncertainty of the theoretical prediction is indicated by the band. The contributions from the renormalization scale uncertainties and the hadronization corrections are added in quadrature.

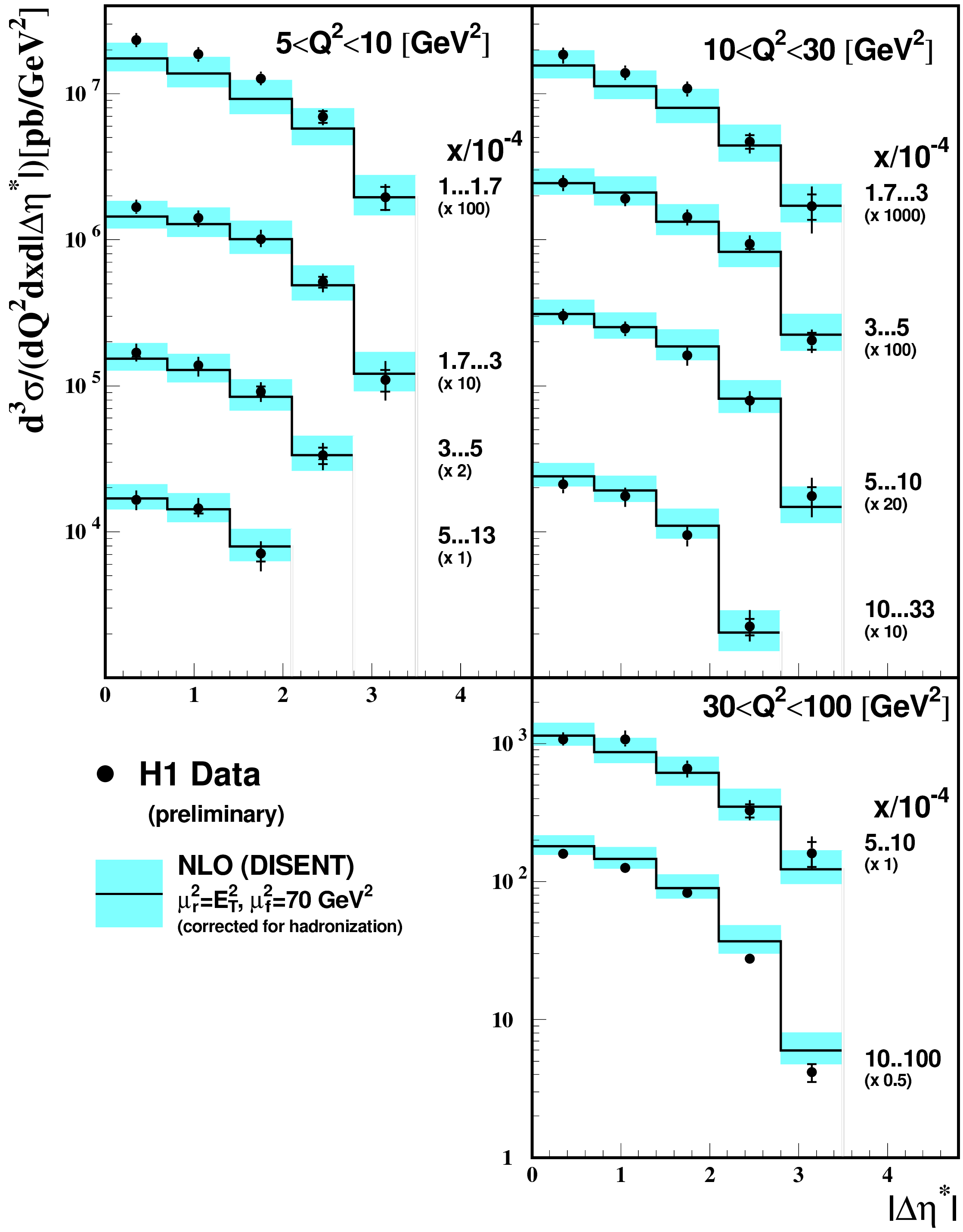

Figure 3: The triple differential inclusive dijet cross section in bins of Bjorken-x and Q^2 as a function of the distance $|\Delta\eta^*|$ between the dijets compared to NLO QCD predictions using the CTEQ6M parton distribution functions. The data are shown together with their statistical (inner error bars) and their statistical and systematic error bars added in quadrature (outer error bars). The NLO predictions are corrected for hadronization effects which lower the pure theoretical prediction by $\approx 10\%$. The error band given for the NLO predictions includes the quadratic sum of hadronization and renormalization scale uncertainties.

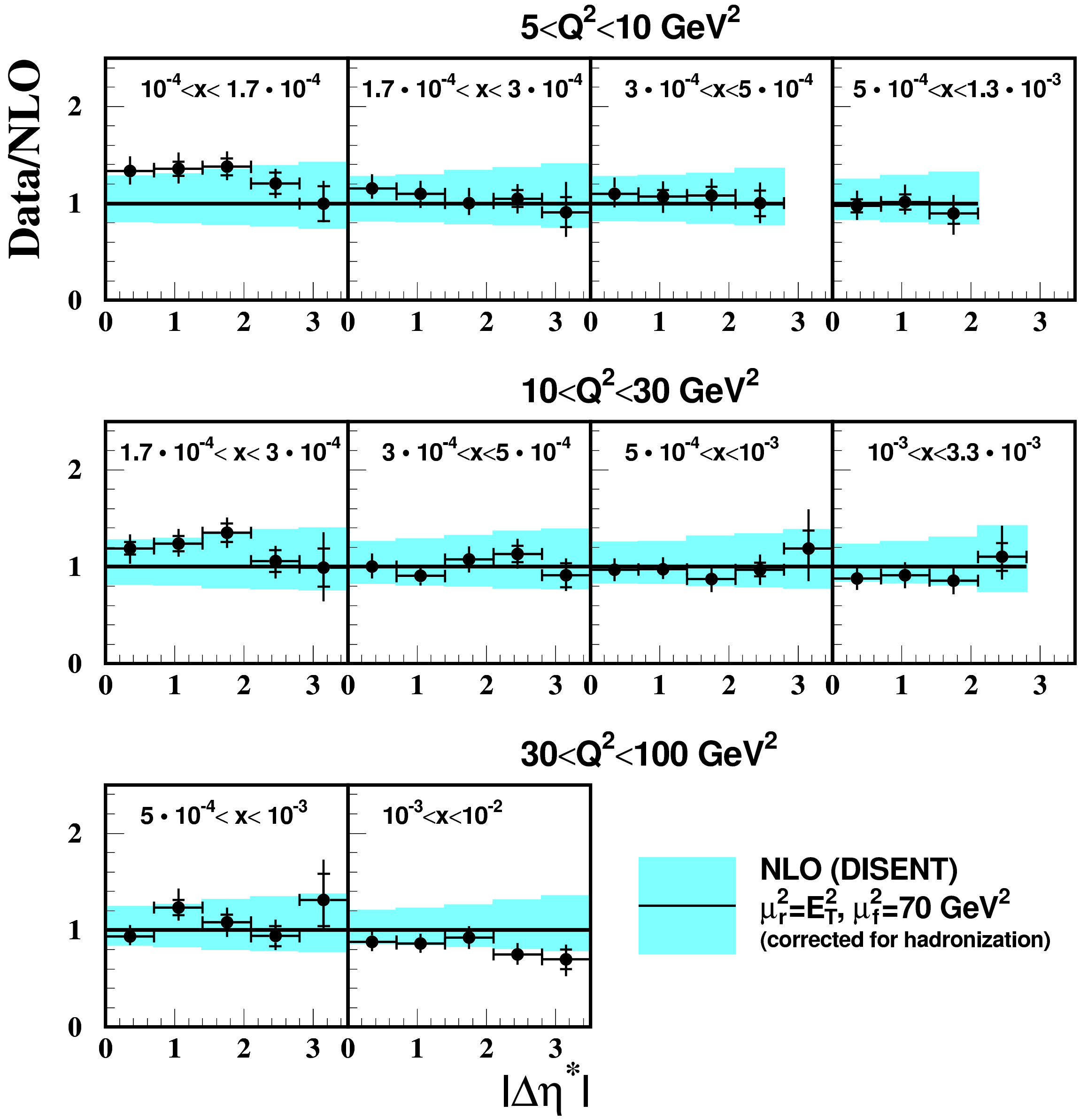

Figure 4: The ratio of the measured triple differential inclusive dijet cross section as a function of the distance $|\Delta\eta^*|$ between the dijets and the NLO QCD predictions using the CTEQ6M parton distribution functions. The uncertainty of the theoretical prediction is indicated by the band. The contributions from the renormalization scale uncertainties and the hadronization corrections are added in quadrature.

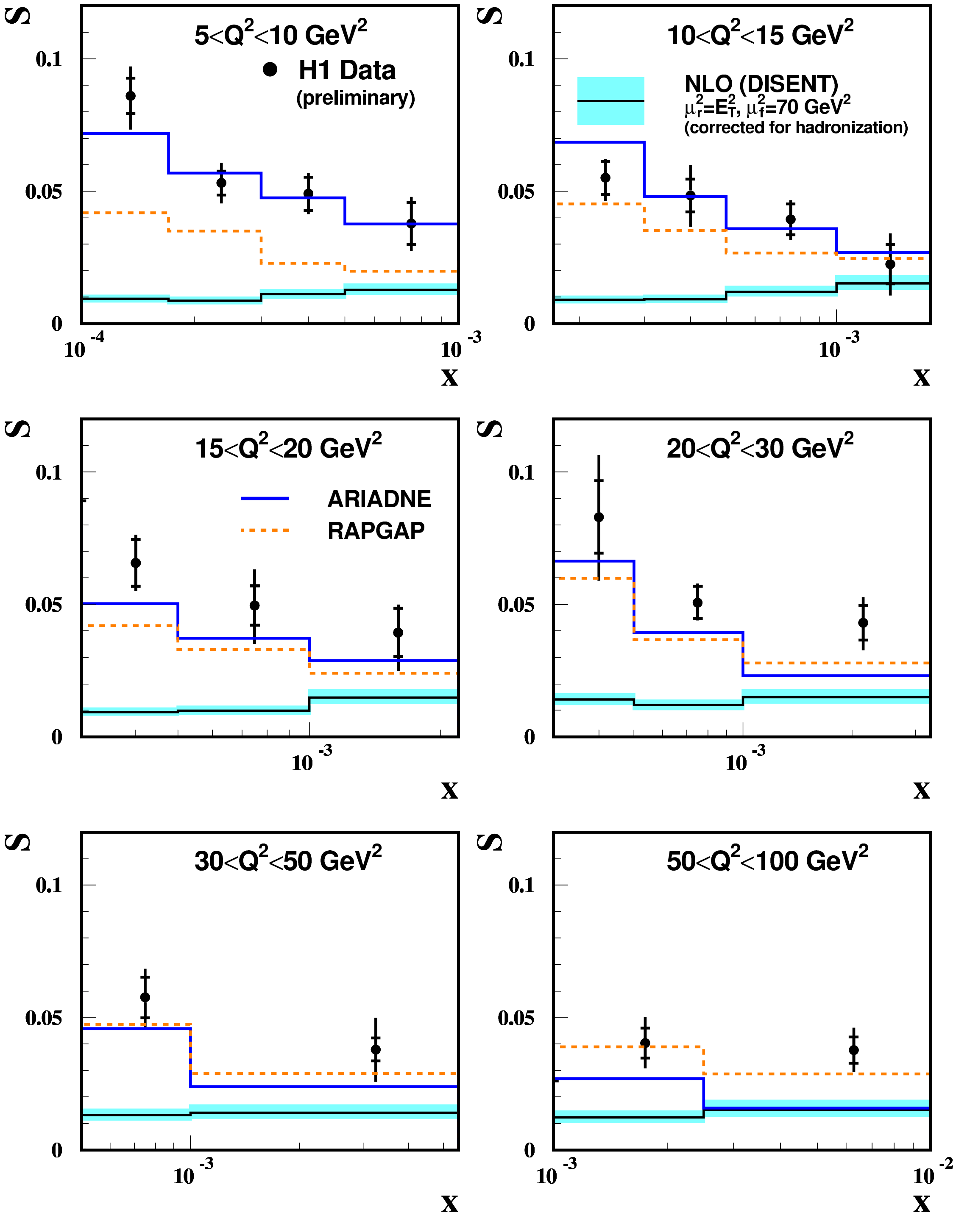

Figure 5: Ratio of jets separated by less than 120° in azimuthal angle to all dijet events as function of Bjorken-x and Q^2 , compared to NLO QCD predictions using the CTEQ6M parton distribution functions and LO QCD models with k_T-ordered (RAPGAP) and with k_T-unordered (ARIADNE) parton showers and full hadronization. The data are shown together with their statistical (inner error bars) and their statistical and systematic error bars added in quadrature (outer error bars). The NLO QCD predictions are represented as error bands including the quadratic sum of hadronization and renormalization scale uncertainties.

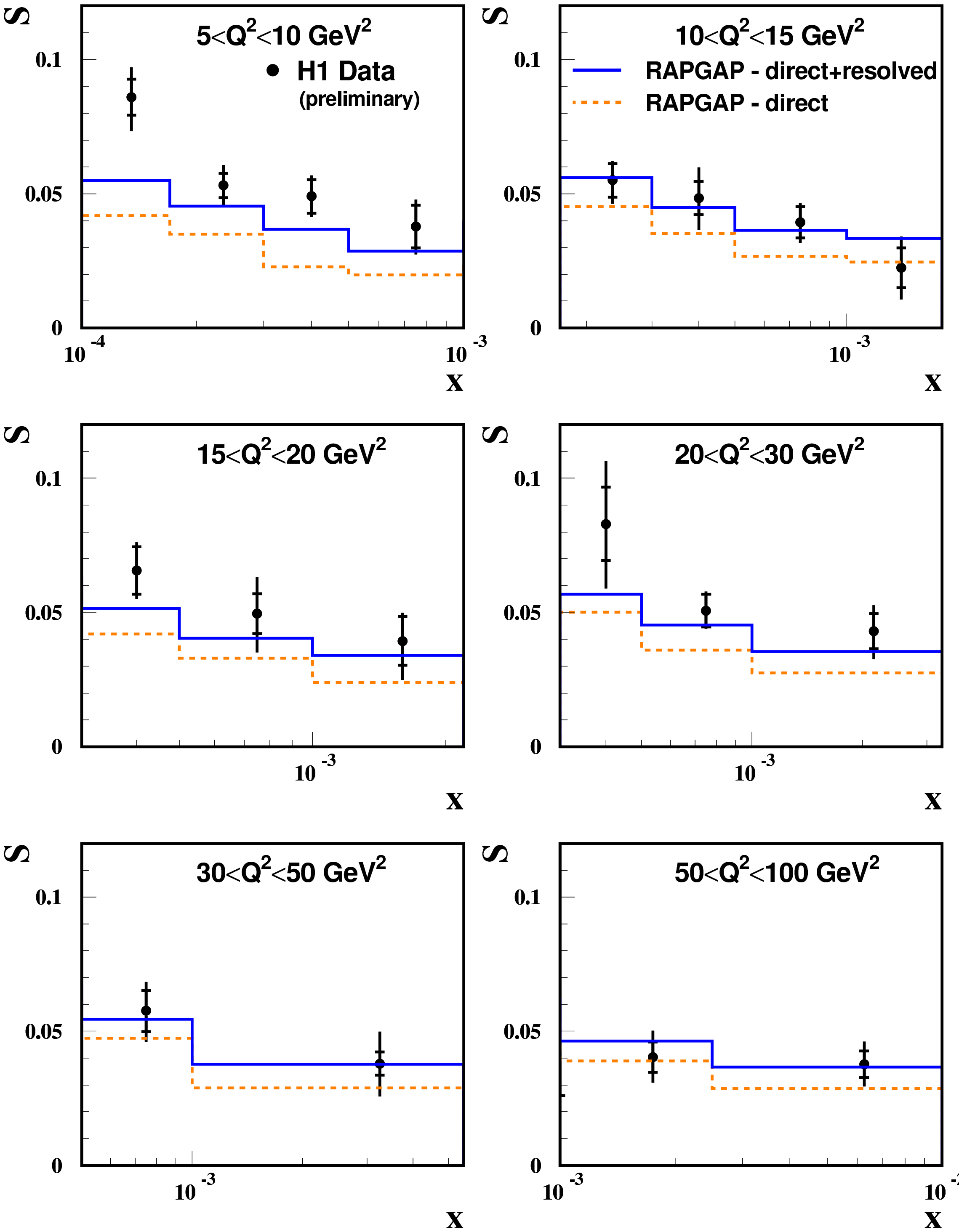

Figure 6: Ratio of jets separated by less than 120° in azimuthal angle to all dijet events as function of Bjorken-x and Q^2. The data are compared to predictions from the RAPGAP Monte Carlo, which allows to include direct alone (full line) and direct and resolved contributions (dashed line) of the virtual photon. The data are shown together with their statistical (inner error bars) and their statistical and systematic error bars added in quadrature (outer error bars).

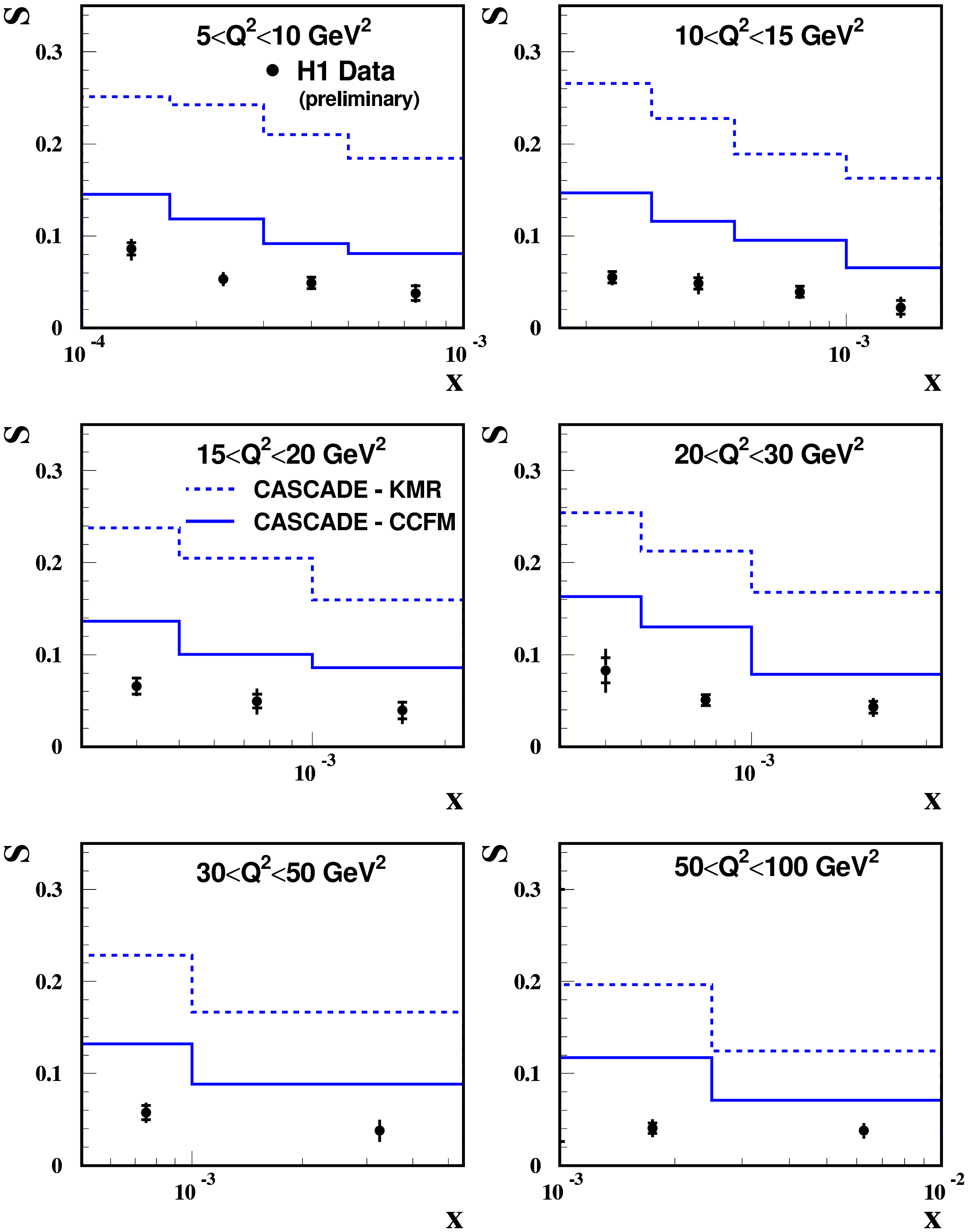

Figure 7: Ratio of jets separated by less than 120° in azimuthal angle to all dijet events as function of Bjorken-x and Q^2. The data are compared to predictions from a QCD model implementing the CCFM evolution (CASCADE) and using the CCFM (full line) and KMR (dashed line) k_t-unintegrated gluon distribution functions. The data are shown together with their statistical (inner error bars) and their statistical and systematic error bars added in quadrature (outer error bars).